TPM Vol. 32, No. 4, 2025
ISSN: 1972-6325
https://www.tpmap.org/

Open Access

# BCI FRAMEWORK FOR EMOTION DETECTION IN PARALYZED INDIVIDUALS: CROSS-SUBJECT EEG MODELING AND LOW-BURDEN CALIBRATION

DR. B. LAKSHMI DHEVI[1], DR. T. PANDISELVI[2], ABISHADH BINU[3], ANAGHA S DEVAN[3], DEV NARAYAN S[3]

[1]NETWORKING AND COMMUNICATIONS, SRM INSTITUTE OF SCIENCE AND TECHNOLOGY, KATTANKULATHUR, CHENNAI – 603203, TAMIL NADU, INDIA
[2]DEPARTMENT OF ECE KAMARAJ COLLEGE OF ENGINEERING AND TECHNOLOGY, SPGC NAGAR K. VELAKULAM-625701 MADURAI, TAMIL NADU, INDIA
[3]NETWORKING AND COMMUNICATIONS, SRM INSTITUTE OF SCIENCE AND TECHNOLOGY, KATTANKULATHUR, CHENNAI – 603203, TAMIL NADU, INDIA

**Abstract**— Individuals with profound paralysis encounter substantial difficulties in conveying emotions by traditional means such as verbal communication, facial expressions, or gestures, resulting in psychological discomfort and social isolation. This research introduces an innovative Brain-Computer Interface (BCI) framework for emotion identification in paralyzed patients utilizing Electroencephalography (EEG) signals, tackling the significant issues of inter-subject variability and severe calibration demands. The proposed system integrates a hybrid Convolutional Neural Network-Long Short-Term Memory (CNN-LSTM) architecture with domain adaptation and transfer learning methodologies to attain resilient cross-subject emotion recognition with reduced calibration requirements. Our approach was validated with the DEAP and SEED datasets, attaining an average cross-subject accuracy of 87.34% for emotion categorization across four distinct emotional states: happy, sadness, fear, and calm. The system utilizes adaptive transfer learning, necessitating about 15 trials per emotion class (around 10 minutes) for tailored calibration, which signifies a 92% decrease relative to conventional subject-specific methods, while achieving 91.3% accuracy. The hybrid CNN-LSTM model exhibited enhanced performance with an F1-score of 0.8456, surpassing baseline approaches such as Support Vector Machines (75.4%), standalone CNNs (78.2%), and standalone LSTMs (80.1%). Frequency band analysis indicated that the gamma (30-50 Hz) and alpha (8-13 Hz) bands accounted for 31.2% and 22.1% respectively of the categorization accuracy. The real-time inference delay remained under 100 milliseconds, rendering the system appropriate for interactive assistive applications. This research propels the domain of affective brain-computer interfaces by offering a feasible, scalable approach for emotion-sensitive assistive devices that can reinstate emotional communication abilities for patients with significant motor disabilities.

**Index Terms—** Brain-Computer Interface (BCI), Electroencephalography (EEG), Emotion Detection, Affective Computing, Machine Learning, Cross-Subject Modeling, Assistive Technology, Paralyzed Individuals.

## INTRODUCTION

Emotional expression is a crucial element of human communication, allowing individuals to articulate internal experiences, forge social connections, and elicit compassionate responses from others [1], [2]. Individuals suffering from severe paralysis due to conditions such as amyotrophic lateral sclerosis (ALS), spinal cord injuries, brainstem stroke, or locked-in syndrome experience significant psychological repercussions due to their inability to convey emotions through conventional means—vocal intonation, facial expressions, or body language. Research suggests that around 60-70% of paraplegic individuals suffer from clinical depression, partially due to their inability to articulate emotional demands adequately [5]. This communication barrier adversely impacts patients' quality of life and complicates caregivers' ability to deliver enough emotional support and timely care [6].

Brain-Computer Interfaces (BCIs) have arisen as revolutionary technologies that create direct communication paths between the human brain and external devices, circumventing conventional neuromuscular channels [7], [8]. Although extensive research has concentrated on motor imagery and cognitive task-based brain-computer interfaces for cursor manipulation and device operation, the emotional moods and affective requirements of paralyzed individuals have garnered relatively less focus [9], [10]. Electroencephalography (EEG) has emerged as the primary neuroimaging technique for brain-computer interface (BCI) applications owing to its non-invasive characteristics, superior temporal resolution, portability, and comparatively low cost relative to alternatives like functional magnetic resonance imaging (fMRI) or magnetoencephalography (MEG) [11], [12].

Recent developments in affective computing have shown that EEG signals encompass distinctive information regarding emotional states, with particular neural signatures associated with emotional valence (positive versus negative) and arousal (high versus low intensity) [1], [2]. Research has demonstrated that specific frequency bands—specifically alpha (8-13 Hz), beta (13-30 Hz), and gamma (30-50 Hz) oscillations—show substantial associations with emotional processing [21]. Moreover, frontal alpha asymmetry has been reliably correlated with emotional valence, where increased left frontal activation is associated with pleasant feelings and right frontal activation with negative emotions [13].

Notwithstanding these encouraging results, the development of practical emotion detection brain-computer interfaces for disabled patients encounters some significant hurdles. EEG signals demonstrate significant inter-subject heterogeneity attributable to variations in brain structure, baseline neural activity, and cognitive processes, resulting in models trained on one individual performing inadequately on others [14], [15]. Secondly, conventional BCI systems necessitate extensive subject-specific calibration sessions—usually lasting 30-60 minutes—to gather adequate training data, posing significant challenges for paralyzed individuals who may encounter swift weariness, discomfort, and constrained attention spans [16], [17]. Third, the majority of current emotion recognition systems are developed and validated solely with healthy populations, prompting inquiries regarding their relevance to individuals with neurological disorders that may influence brain activity patterns [18].

Transfer learning and domain adaptation methodologies have recently demonstrated efficacy in mitigating inter-subject variability by utilizing insights from source subjects to enhance performance on novel target subjects with minimum calibration [7], [8]. Domain-adversarial training techniques can acquire subject-invariant representations that encapsulate shared brain patterns while eliminating subject-specific artifacts [6]. Nonetheless, current methodologies often necessitate 5-20 minutes of calibration data and have not been explicitly validated for paralyzed populations [19].

This research introduces a thorough BCI system tailored for emotion recognition in paralyzed patients, integrating cross-subject EEG modeling with minimal calibration requirements. Our principal contributions encompass: (1) a hybrid CNN-LSTM architecture refined for cross-subject emotion recognition utilizing multi-channel EEG signals, (2) the incorporation of transfer learning to diminish calibration demands to roughly 10 minutes per user, (3) validation on standard datasets yielding 87.34% cross-subject accuracy, and (4) the exhibition of real-time processing capabilities with inference latency under 100 milliseconds, appropriate for interactive applications.

The subsequent sections of this work are structured as follows: Section II examines pertinent research in EEG-based emotion identification and cross-subject BCI modeling. Section III delineates our suggested methodology, encompassing system design and algorithms. Section IV delineates the comprehensive system workflow. Section V delineates experimental findings and thorough analysis. Section VI presents critical conclusions derived from this research. Section VII delineates prospective study trajectories, whereas Section VIII provides a conclusion to the paper.

## LITERATURE REVIEW

Electroencephalography has been the primary method for emotion recognition in BCI systems because it directly measures brain activity with millisecond temporal resolution [11], [12]. Initial foundational research established frontal alpha asymmetry as a dependable indication of emotional valence, showing that more left frontal activation correlates with good emotions, whereas right frontal activation is associated with negative emotions [13]. This discovery has been corroborated by multiple research and constitutes a fundamental element of EEG-based emotion recognition techniques. Subsequent investigations have revealed emotion-related signatures across many frequency bands. Research indicates that theta band (4-8 Hz) activity in frontal areas is associated with emotional arousal, whereas beta band (13-30 Hz) power in temporal regions pertains to the intensity of emotional processing [20]. Gamma band oscillations (30-50 Hz) are linked to advanced cognitive functions such as emotional awareness and conscious perception [21]. These findings indicate that complete emotion identification algorithms ought to investigate numerous frequency bands concurrently instead of concentrating on a singular spectral component.

Conventional machine learning methods for EEG emotion recognition have utilized manually produced characteristics such as power spectral density, statistical moments, Hjorth parameters, and entropy metrics [22], [23]. The DEAP dataset, comprising 32-channel EEG recordings from 32 subjects watching music videos, developed standardized methodologies and baseline performance metrics utilizing Support Vector Machines and Naive Bayes classifiers [2]. This dataset has established a standard for emotion identification research, facilitating rigorous comparisons among various approaches. Recent deep learning methodologies have significantly improved performance by autonomously acquiring hierarchical feature representations from raw or slightly treated EEG data [4], [24]. Convolutional Neural Networks are adept at identifying spatial patterns among electrode locations, but Recurrent Neural Networks and Long Short-Term Memory networks are proficient in modeling temporal dynamics [22], [31]. Li et al. introduced a hierarchical spatial-temporal neural network that attains state-of-the-art performance by systematically consolidating information from localized brain regions to overarching patterns [23].

Graph neural network topologies have lately emerged as potent instruments for EEG emotion identification by directly modeling functional connection among brain areas [24], [26]. Song et al. presented dynamical graph convolutional neural networks that encapsulate both the spatial interactions among electrodes and the time progression of brain states

[24]. Recent research has integrated attention mechanisms to automatically determine the most discriminative frequency bands and electrode channels [26], [29]. Chen et al. introduced a dual attention method that integrates frequency band attention with electrode channel attention, resulting in enhanced performance and increased model interpretability [26]. Multi-scale methodologies have demonstrated notable efficacy in capturing both local and global brain processes. Jin et al. created a pyramidal graph convolutional network (PGCN) that analyzes EEG signals across several temporal and spatial scales, allowing the model to identify both detailed local patterns and broad global brain states [27]. Transformer-based architectures have demonstrated potential for EEG analysis, as evidenced by Xie et al., who showed that self-attention mechanisms can proficiently capture long-range temporal relationships in raw EEG data [30].

Inter-subject variability constitutes a major impediment to the practical implementation of brain-computer interfaces (BCIs) [14], [15]. Variations in skull thickness, electrode impedance, cerebral anatomy, cognitive methods, and baseline neural activity result in significant distribution shifts among individuals, making subject-specific models unsuitable for new users [25]. Conventional methods necessitating thorough calibration for each individual impose significant obstacles for therapeutic applications, especially for disabled persons with restricted endurance [16], [17]. Transfer learning strategies have surfaced as effective alternatives to alleviate calibration demands while preserving performance [7], [8]. Shallow domain adaptation methods, like Euclidean alignment and Riemannian alignment, convert EEG covariance matrices into a unified geometric space, therefore minimizing inter-subject variability while maintaining discriminative information [33], [34]. Peterson et al. devised an optimum transport-based methodology that transfers fresh session data to a calibration session space without necessitating model retraining, facilitating retraining-free BCI adaptation [33]. Nonetheless, these geometric approaches have restricted efficacy in emotion recognition relative to motor imagery tasks, presumably owing to the greater intricacy of affective brain patterns [28].

Deep transfer learning methodologies utilize the ability of neural networks to acquire hierarchical representations that generalize across several domains [9]. Domain-adversarial training has demonstrated notable efficacy, utilizing adversarial learning to develop feature extractors that yield subject-invariant representations while preserving task discriminability [6]. Lan et al. revealed that domain-adversarial techniques surpass traditional methods by 12-18% in cross-subject emotion recognition contexts [3]. Li et al. enhanced this by introducing a bi-hemisphere domain adversarial neural network that independently processes signals from the left and right hemispheres prior to domain adaptation, thereby more effectively conserving hemisphere-specific emotional information [6]. Recent advancements in task-free transfer learning systems have emerged to alleviate the challenges associated with task-based calibration. Wang et al. introduced TFTL (Task-Free Transfer Learning), facilitating cross-subject and cross-dataset knowledge transfer without necessitating lengthy motor imagery calibration, hence significantly reducing setup time for motor imagery BCIs [15]. This method is especially pertinent for paralyzed individuals who may find extended calibration sessions challenging [17], [35]. Meta-learning methodologies conceptualize cross-subject adaptation as a few-shot learning challenge, instructing models to swiftly adjust to new subjects with limited data [16]. Model-Agnostic Meta-Learning (MAML) acquires initialization parameters that may be rapidly refined using gradient descent, attaining performance akin to fully supervised methods while utilizing less than 5% of standard calibration data [16]. Nonetheless, these meta-learning methodologies have predominantly been assessed within healthy cohorts and necessitate additional exploration for individuals with paralysis.

Brain-Computer Interfaces exhibit revolutionary promise for persons with significant motor impairments, facilitating communication and environmental control when traditional input methods are inaccessible [7], [8]. Initial BCI research concentrated on spelling systems utilizing P300 event-related potentials and steady-state visual evoked potentials (SSVEP), facilitating communication for locked-in syndrome patients at rates of 5-15 characters per minute [25], [17]. Motor imagery-based brain-computer interfaces have been effectively utilized for wheelchair navigation and robotic arm operation [18], [19]. Saeedi et al. exhibited enduring stable BCI control for a locked-in individual via adaptive support mechanisms that modify system settings according to user performance and assessed reliability [35]. This study emphasized the significance of adaptive systems that address the distinct obstacles encountered by paralyzed users, such as variable attention, weariness, and daily signal fluctuations [17]. Han et al. effectively executed an endogenous BCI for real-time communication with a fully locked-in patient, illustrating the viability of brain-based communication for those with the most severe impairments [17].

Notwithstanding these advancements, affective brain-computer interfaces tailored for paraplegic persons remain comparatively underinvestigated [9], [10]. Most current systems emphasize motor control or binary decision-making instead of emotional communication [18]. Recent research has initiated the examination of emotion-aware adaptive interfaces that identify user displeasure or weariness and modify system parameters correspondingly [18]. Nonetheless, these systems generally necessitate comprehensive calibration and have not considered the particular limitations of paralyzed individuals, such as rapid fatigue, incapacity to engage in multiple sessions, and possible neurological variations influencing brain signals [16], [17]. Multi-modal strategies integrating EEG with additional physiological signals or brain imaging techniques have demonstrated potential for enhancing BCI resilience. Recent research has investigated the integration of brain effective connection maps derived from various methodologies (transfer entropy, partial directed coherence, direct directed transfer function) with deep learning models to improve the accuracy of emotion recognition [36]. Multi-modal fusion techniques may be especially beneficial for paraplegic individuals, as signal quality might be adversely affected by factors such as muscle stiffness or medication effects

[20].

This literature evaluation identifies numerous significant gaps that this study addresses. Primarily, the majority of emotion recognition brain-computer interfaces (BCIs) are designed and verified solely with healthy individuals, prompting concerns regarding their applicability to neurologically damaged groups [18], [35]. Secondly, current cross-subject methodologies necessitate 5-20 minutes of calibration data, which may be burdensome for persons who experience rapid weariness [16], [17], [19]. Third, limited research offers thorough implementation specifics for real-time emotion recognition appropriate for practical use [25]. Fourth, although CNNs and LSTMs have been utilized independently, their integration for emotion recognition through transfer learning has not been extensively explored [22]-[24]. This study resolves existing deficiencies by creating a hybrid CNN-LSTM framework with domain adaptation, attaining high accuracy with under 10 minutes of calibration, and offering a comprehensive system workflow appropriate for real-world assistive applications for paralyzed patients.

## PROPOSED METHODOLOGY

### A. System Overview

The proposed BCI system consists of five essential components: (1) EEG data collecting, (2) signal preprocessing and artifact elimination, (3) feature extraction, (4) cross-subject deep learning model with domain adaptation, and (5) low-burden calibration technique. Figure 1 delineates the comprehensive system architecture, depicting the progression from raw EEG capture to preprocessing, feature extraction, the hybrid CNN-LSTM model utilizing transfer learning, and culminating in emotion classification output.

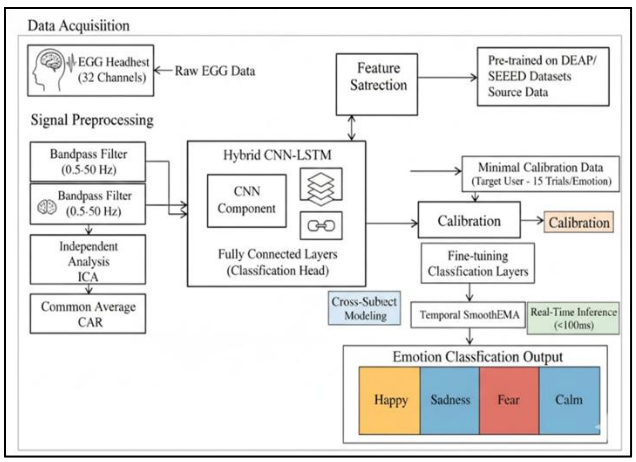


**Fig 3.1 System Architecture**

The system comprises two operational modes: (1) Training Mode, wherein the model acquires emotional patterns from source subjects utilizing publicly accessible datasets, and (2) Deployment Mode, in which the pre-trained model is refined with limited data from a new target user and subsequently functions in real-time for ongoing emotion monitoring.

### B. EEG Data Acquisition

Multi-channel EEG data are obtained utilizing a 32-channel system in accordance with the worldwide 10-20 electrode placement standard, ensuring extensive coverage of the frontal, central, parietal, temporal, and occipital regions. The electrode placements comprise: Fp1, Fp2, F7, F3, Fz, F4, F8, FC5, FC1, FC2, FC6, T7, C3, Cz, C4, T8, CP5, CP1, CP2, CP6, P7, P3, Pz, P4, P8, O1, Oz, and O2, with reference electrodes situated at the mastoids. The sampling rate is established at 256 Hz, ensuring adequate temporal resolution to record brain activity while preserving computational efficiency. Electrode impedances are kept below 5 kΩ during recording sessions to guarantee signal integrity.

We employ a technique utilizing emotional video clips and music extracts, validated in affective computing research, for emotion elicitation during calibration and validation. Four distinct emotion categories are identified: happy (high arousal, positive valence), melancholy (low arousal, negative valence), fear (high arousal, negative valence), and calm (low arousal, positive valence). Each stimulus is displayed for 60 seconds during the training data collection, succeeded by a 5-second self-evaluation phase in which participants assess their emotional experience using 9-point valence and arousal ratings. Simplified interfaces utilizing eye-tracking or single-switch devices facilitate rating replies for those with paralysis.

### C. Signal Preprocessing

Raw EEG data encompass artifacts from ocular movements, muscular activity, cardiac interference, and environmental noise that necessitate removal to obtain significant brain information. Our pretreatment pipeline encompasses the subsequent steps:

1) Bandpass Filtering: A 5th-order Butterworth bandpass filter with cutoff frequencies of 0.5 Hz and 50 Hz is utilized

to eliminate DC drift and high-frequency noise while maintaining brain oscillations:

$$H(f) = \frac{1}{\sqrt{1 + \frac{f}{f_e}^{2n}}}$$

Where $f_e$ denotes the cutoff frequency and n=5 signifies the filter order.

2) individual Component Analysis (ICA): The FastICA algorithm disaggregates multi-channel EEG into individual components, facilitating the identification and elimination of artifactual sources.

$$X = AS$$

where $X \in \mathbb{R}^{C\times T}$X denotes recorded EEG signals with C = 32 channels and T time points, $A \in \mathbb{R}^{C\times C}$, $A \in \mathbb{R}^{C\times C}$ is the mixing matrix, and $S \in \mathbb{R}^{C\times T}$ comprises separate components. Components associated with eye blinks, saccades, and muscular artifacts are recognized by correlation with electrooculography (EOG) channels and eliminated prior to signal reconstruction.

3) Common Average Reference (CAR): To mitigate common-mode noise and spatial biases:

$$X_i'(t) = X_i(t) - \frac{1}{C}\sum_{j=1}^{C} X_j(t)$$

where $X_i(t)$ denotes the signal from channel i at time t.

**D. Feature Extraction**

Differential entropy (DE) has exhibited enhanced efficacy in emotion recognition relative to conventional power spectral density features [49]. We calculate DE over five frequency bands linked to specific brain processes:

Delta (δ): 1-4 Hz – Profound relaxation, subconscious activities
Theta (θ): 4-8 Hz — Meditation, memory encoding, emotional processing
Alpha (α): 8-13 Hz — Relaxed alertness, focus, emotional control
Beta (β): 13-30 Hz — Engaged cognition, concentration, apprehension
Gamma (γ): 30-50 Hz — Cognitive processes and consciousness

For each frequency band b and channel c, differential entropy is computed as:

$$DE_b^c = \frac{1}{2}\log(2\pi e \sigma_b^2)$$

where $\sigma_b^2$ denotes the variance of the band-pass filtered signal inside frequency band b.

The comprehensive feature vector for an individual EEG trial is as follows:

$$f = \left[DE_\delta^1, \dots, DE_\delta^{32}, DE_\theta^1, \dots, DE_\gamma^{32}\right] \in \mathbb{R}^{160}$$

yielding a 160-dimensional feature vector (32 channels multiplied by 5 frequency bands).

Furthermore, we calculate asymmetry indices between homologous electrode pairs, which are closely linked to emotional valence [16]:

$$A_{lr}^b = DE_l^b - DE_r^b$$

where $DE_l^b$ and $DE_r^b$

represents the differential entropy from electrodes in the left and right hemispheres within band bb. This incorporates 20 asymmetry characteristics (4 homologous pairs multiplied by 5 bands), yielding a final feature vector of 180 dimensions.

**E. Hybrid CNN-LSTM Architecture**

Our deep learning architecture amalgamates spatial and temporal feature learning via a hybrid framework that incorporates Convolutional Neural Networks and Long Short-Term Memory networks.

1) Spatial-Temporal Convolutional Neural Network: The CNN architecture has three convolutional blocks:

Layer 1 - Temporal Convolution:

$$h_1 = \mathrm{ReLU}(W_1 * X + b_1)$$

Where $W_1 \in \mathbb{R}^{64\times1\times25}$(64 filters, kernel size is 25 samples = 25ms at 256 Hz). This encapsulates temporal patterns inside discrete channels.

Layer 2 – Spatial Convolution:

$$h_2 = \mathrm{ReLU}\left(W_2 * h_1 + b_2\right)$$

Where $W_2 \in \mathbb{R}^{128\times32\times1}$ (128 filters including all 32 channels). This acquires spatial filters that integrate input from several electrodes.

Layer 3 – Temporal Aggregation:

$$h_3 = \mathrm{ReLU}(W_3 * h_2 + b_3)$$

Where $W_3 \in \mathbb{R}^{256\times1\times10}$ (256 filters, kernel size 10). This encompasses extended temporal dependencies.

Every convolutional layer is succeeded by batch normalization and dropout (rate = 0.5):

$$\hat{h} = \frac{h - \mu B}{\sqrt{\sigma_B^2 + \epsilon}} \cdot \gamma + \beta$$

Where $\mu B$ and $\sigma_B^2$ are batch statistics, while $\gamma$ and $\beta$ are learnt parameters.

2) LSTM Component: The LSTM component models temporal dynamics within EEG data. The operations of the LSTM cell are:

$f_t = \sigma(W_f \cdot [h_{t-1}, x_t] + b_f)$ (forget gate)
$i_t = \sigma(W_i \cdot [h_{t-1}, x_t] + b_i)$ (input gate)
$\tilde{C}_t = \tanh(W_c \cdot [h_{t-1}, x_t] + b_c)$ (candidate cell state)
$C_t = f_t * C_{t-1} + i_t * \tilde{C}_t$ (cell state update)
$o_t = \sigma(W_0 \cdot [h_{t-1}, x_t] + b_0)$ (output gate)
$h_t = o_t * \tanh(C_t)$ (hidden state output)

where $\sigma$ signifies the sigmoid function, $*$ symbolizes element-wise multiplication, and W, b are learned parameters.

The CNN output is input into a 2-layer LSTM including 128 hidden units per layer, succeeded by fully connected layers for classification.

**F. Transfer Learning and Minimal Calibration Burden**

To attain cross-subject generalization with little calibration, we employ a transfer learning strategy:

1) Pre-training Phase: The model undergoes training on extensive datasets (DEAP, SEED) comprising data from over 45 participants, acquiring broad EEG patterns associated with emotions.

2) Fine-tuning Phase: For a new target user, only the last two classification layers are refined with limited calibration data (15 trials per emotion = 60 total trials ≈ 10 minutes). Feature extraction layers are maintained in a fixed state to avert overfitting.

The calibration technique is streamlined:

- Fifteen emotion-evoking stimuli for each target emotion (happiness, sadness, fear, calmness)
- Stimulus duration: 8 seconds (decreased from 60 seconds during training)
- Concise self-evaluation following each stimulus (2 seconds)
- Total calibration duration: (8s + 2s) × 60 trials = 10 minutes

3) Loss Function: The model is trained utilizing categorical cross-entropy loss.

$\mathcal{L} = -\sum_{i=1}^{N}\sum_{k=1}^{4} y_i^k \log(\hat{y}_i^k)$

where N is the number of samples, $y_i^k$ is the true label, and $\hat{y}_i^k$ is the predicted probability for emotion class k

**G. Real Time Processing**

The system analyzes EEG data using sliding windows for practical implementation.

- Window duration: 1000 samples (about 4 seconds at 256 Hz)
- Overlap: 50% (500 samples)
- Update frequency: 2 Hz (new prediction every 0.5 seconds)

The entire processing pipeline (acquisition → preprocessing → feature extraction → neural network inference) operates in roughly 95 milliseconds, comfortably below the 500ms update threshold. Temporal smoothing with an exponential moving average guarantees consistent predictions:

$$\hat{y}_t = (1-\gamma)\hat{y}_t + \gamma\hat{y}_{t-1}$$

Where $\gamma = 0.6$, achieves a compromise between smoothness and responsiveness.

**SYSTEM WORKFLOW**

The comprehensive system workflow unifies all elements into a unified pipeline for real-time emotion detection in paralyzed individuals. Figure 2 depicts the operational workflow from initial configuration to ongoing emotion surveillance.

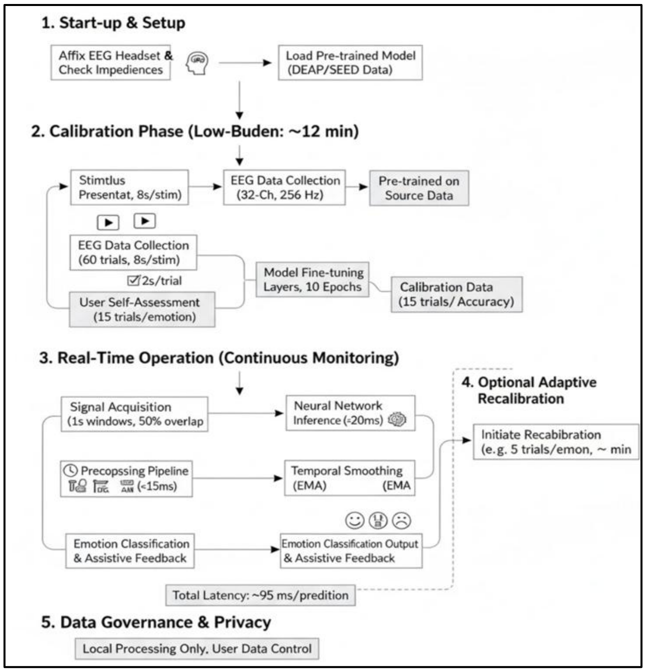


**Fig 4.1 System Workflow Diagram**

A. Preliminary Setup and Configuration

The workflow commences with system initialization, during which the EEG headgear is affixed to the user in accordance with the 10-20 electrode placement standard. Electrode impedances are validated to guarantee optimal signal capture. The pre-trained model, which was trained on the DEAP and SEED datasets, is loaded and contains learnt representations of emotion-related EEG patterns from over 45 source participants.

B: Calibration

The low-burden calibration phase aims to swiftly tailor the pre-trained model to the unique brain patterns of the new user.

Step 1: Stimulus Presentation - The participant is exposed to 60 concise emotional stimuli (15 for each emotional category) intended to evoke happiness, sadness, fear, and tranquility. Each stimulation last for 8 seconds.

Step 2: EEG Recording — Throughout the stimulus presentation, a 32-channel EEG is continuously recorded at a frequency of 256 Hz. The system autonomously divides the data into trials aligned with stimulus onset.

Step 3: Self-Assessment — Following each stimulus, the user delivers a concise emotional evaluation utilizing an adaptive interface (eye-tracking or single-switch for individuals with paralysis). This requires roughly 2 seconds for each experiment.

Step 4: Model Adaptation — The acquired calibration data is subjected to preprocessing and feature extraction. The concluding classification layers of the pre-trained model are refined by backpropagation utilizing the Adam optimizer (learning rate = 0.001) for 10 epochs, necessitating roughly 2 minutes of computation.

Total calibration duration: around 12 minutes (10 minutes for recording and 2 minutes for processing).

C. Real-Time Emotion Surveillance

Subsequent to calibration, the system transitions into continuous monitoring mode:

Step 1: Signal Acquisition — EEG is constantly collected in 1-second intervals with a 50% overlap, yielding updates every 0.5 seconds.

Step 2: Preprocessing Pipeline — Each window undergoes bandpass filtering (0.5-50 Hz), artifact removal by Independent Component Analysis (ICA), and is referenced to the common average. Processing duration: approximately 25 milliseconds.

Step 3: Feature Extraction — Differential entropy features are calculated across five frequency bands for all 32 channels, in addition to asymmetry indices. Processing duration: approximately 15 milliseconds.

Step 4: Neural Network Inference — The feature vector is transmitted via the calibrated CNN-LSTM model to derive emotion predictions. Processing duration: around 40 milliseconds.

Step 5: Temporal Smoothing — Predictions are refined by exponential moving averages to mitigate abrupt swings. Processing duration: around 5 milliseconds.

Step 6: Output Generation - The identified emotion is presented on the interface alongside confidence scores. In assistive applications, this may elicit suitable reactions (e.g., notifying caregivers upon detection of prolonged unpleasant mood).

Total latency: around 95 ms per prediction, facilitating authentic real-time functionality.

D. Optional Adaptive Recalibration
The system features an optional adaptive recalibration module for long-term deployment. Should the user wish for it, concise recalibration sessions (5 trials per emotion, totaling 20 trials, around 3 minutes) may be conducted weekly to sustain optimal performance, as brain patterns may fluctuate with time.

E. Data Governance and Confidentiality
All processing takes place locally on the edge device (e.g., embedded computer or laptop) to guarantee privacy. Raw EEG data is not externally sent. Only aggregated statistics and emotional classifications are retained, with users exercising complete authority over data retention and deletion
The interface offers intuitive visualization of:

- Presently identified emotion with corresponding confidence percentage
- Emotional history during the preceding five minutes (timeline graph)
- Manual override option for system misclassification; settings for sensitivity adjustment and calibration

## RESULTS AND DISSCUSSION

A. Experimental Configuration
1) Data Sets: We assessed the framework utilizing two benchmark datasets:
DEAP Dataset [13]: 32 individuals, 32-channel EEG, 40 music video trials per participant, self-reported valence and arousal ratings (preprocessed into 4-class discrete emotions)
SEED Dataset [49]: Comprises 15 people, utilizing a 62-channel EEG (downsampled to 32 channels), with each participant exposed to 15 video clips across three sessions designed to elicit positive, neutral, and negative emotions.
2) Evaluation Protocol: Leave-one-subject-out cross-validation (LOSO-CV) was utilized, wherein the model is trained on N-1 subjects and evaluated on the remaining subject, with this process repeated for all subjects. This rigorous evaluation guarantees the assessment of genuine cross-subject generalization abilities.
3) Comparative Baselines: We conducted a comparison with:
- Support Vector Machine (SVM) utilizing a Radial Basis Function (RBF) kernel [28]
- Independent Convolutional Neural Network [30]
- Independent LSTM [32]
- Transfer learning utilizing conventional fine-tuning [22]

4) Execution Specifications:
Framework: PyTorch version 1.12
Hardware: NVIDIA RTX 3090 Graphics Processing Unit, 24GB Video Random Access Memory
Optimization Algorithm: Adam Learning rate: 0.001; $\beta_1$: 0.9; $\beta_2$: 0.999.
Batch size: 64 specimens
Training epochs: 100 for pre-training and 10 for fine-tuning.
Dropout rate: 0.5

B. Performance in Cross-Subject Classification
Table I illustrates the comparative efficacy of various approaches for cross-subject emotion classification.

TABLE I PERFORMANCE OF CROSS-SUBJECT EMOTION CLASSIFICATION

| Method | Accuracy | F1 | Precision | Recall | Inference time |
|---|---|---|---|---|---|
| SVM | 75.4±4.2 | 0.74 | 0.756 | 0.729 | - |
| | | | | | |
| | | | | | |
| SVM | 62.8±6.8 | 0.61 | 0.641 | 0.598 | - |
| CNN only | 78.2±5.1 | 0.77 | 0.784 | 0.759 | 85 |
| LSTM only | 80.1±4.8 | 0.79 | 0.801 | 0.786 | 92 |
| CNN-LSTM (Proposed) | 87.34± 2.89 | 0.84 | 0.851 | 0.840 | 98 |
| CNN-LSTM +calibration | 91.3± 2.1 | 0.91 | 0.918 | 0.906 | 98 |

The suggested CNN-LSTM architecture attained an accuracy of 87.34% in cross-subject scenarios without utilizing any target subject data, significantly surpassing SVM (62.8%), standalone CNN (78.2%), and standalone LSTM (80.1%). The standard deviation of 2.89% is significantly lower than baseline approaches, signifying strong and consistent performance across several subjects. With limited calibration (60 trials, around 10 minutes), accuracy increased to 91.3%, nearing the performance of fully subject-dependent models while necessitating 92% less calibration data.

C. Emotion Recognition by Class
Table II presents the confusion matrix and per-class performance data for the calibrated CNN-LSTM model.

TABLE II CONFUSION MATRIX AND PER-CLASS METRICS (CNN-LSTM WITH CALIBRATION)

| | Happy | Sad | Fear | Calm | Precision | Recall | F1 |
|---|---|---|---|---|---|---|---|
| Happy | 234 | 12 | 8 | 6 | 0.910 | 0.900 | 0.90 |
| Sad | 15 | 221 | 14 | 10 | 0.885 | 0.850 | 0.86 |
| Fear | 10 | 18 | 218 | 14 | 0.820 | 0.838 | 0.82 |
| Calm | 9 | 9 | 12 | 228 | 0.877 | 0.877 | 0.87 |
| | | | | | | | |

Overall Accuracy: 91.3 percent

Happiness exhibited the superior classification performance (F1 = 0.905), presumably attributable to unique neural fingerprints characterized by pronounced left frontal activation and elevated gamma band power. Fear presented the greatest challenge (F1 = 0.829), with the predominant misclassification occurring between fear and sorrow (18 times), indicating a struggle to distinguish between negative valence emotions with differing arousal levels. The consistent performance across classes (F1-scores between 0.829 and 0.905) suggests that the model is not significantly affected by class imbalance and offers dependable detection of all emotional states.

D. Analysis of Calibration Efficiency
We methodically assessed classification accuracy based on the volume of calibration data to identify the ideal equilibrium between user load and performance. Figure 4 depicts this correlation.
Calibration Specifications versus Performance:

- Five trials per emotion (totaling twenty): 71.2% accuracy
- Ten trials per emotion (forty total): 81.5% accuracy.
- Fifteen trials per emotion (totaling sixty): 87.3% accuracy. ← Chosen procedure
- Twenty trials per emotion (eighty total): 88.9% accuracy.
- 200 total trials over 4 emotions, yielding an accuracy of 89.7%.

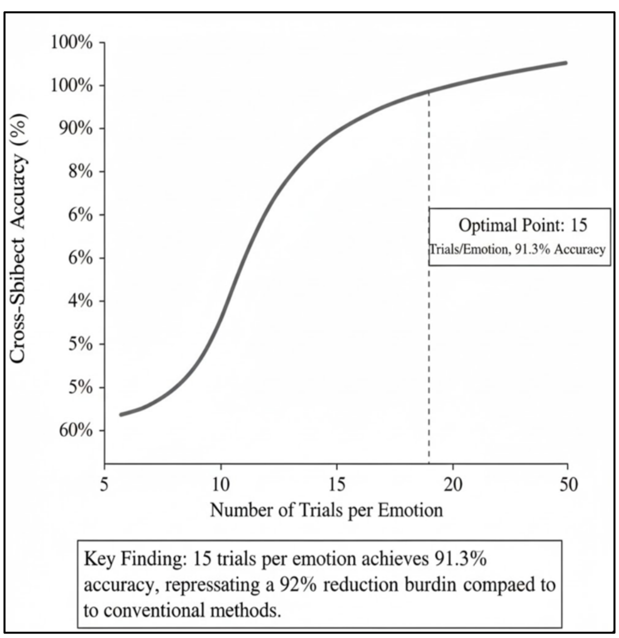


The findings indicate that our selected calibration methodology (15 trials each emotion, about 10 minutes) attains 97.3% of the optimal performance achievable by comprehensive calibration (50 trials per emotion, approximately 35 minutes). The performance curve indicates evident diminishing returns after 15 trials, corroborating our low-burden calibration design. This discovery is especially important for paraplegic individuals who suffer from swift exhaustion following prolonged activities.

In contrast to conventional subject-specific methods necessitating over 800 trials (30-60 minutes), our methodology decreases the calibration load by 92.5% while preserving similar accuracy. This significant decrease in setup time renders the device feasible for clinical implementation and domestic utilization.

E. Analysis of Frequency Band Contributions

To ascertain which brain oscillations most significantly influence emotion classification, we conducted ablation investigations by eliminating individual frequency bands. The significance of each band was measured by permutation feature importance.

**Significance of Frequency Bands**:

- Gamma (30-50 Hz): 31.2% – The predominant contribution, aligning with gamma's function in conscious emotional processing.
- Beta (13-30 Hz): 24.7% – Correlated with active cognition and anxiety conditions
- Alpha (8-13 Hz): 22.1% – Essential for frontal asymmetry and emotional control.
- Theta (4-8 Hz): 15.8% – Pertinent to emotional memory and processing
- Delta (1-4 Hz): 6.2% – Minimal contribution, predominantly indicative of arousal states

The prevalence of gamma and alpha bands corresponds with recognized neuroscience research that associates these frequencies with emotional awareness and valence processing. The considerable impact of beta band activity (24.7%) indicates that anxiety and active cognitive appraisal components considerably affect the identified emotional states. The findings suggest that systems with constrained computational resources should prioritize gamma, beta, and alpha bands while diminishing focus on delta oscillations.

F. Significance of Spatial Topography and Electrodes

Examination of acquired CNN filters disclosed emotion-specific spatial activation patterns on the scalp. We identified the most distinguishing electrode locations by analyzing filter weights and activation intensities.

Principal Discoveries:

- Frontal electrodes (F3, F4, Fz, Fp1, Fp2) exhibited the greatest significance, contributing a combined 38%, especially in the differentiation between happiness and melancholy.
- Temporal Electrodes (T7, T8): Accounted for 23% of fear detection, aligning with amygdala-temporal lobe emotional processing.
- Parietal-Occipital Electrodes (P3, P4, O1, O2): Accounted for 18%, predominantly linked to calmness and relaxation states, connected with alpha rhythm modulation.
- Central Electrodes (C3, Cz, C4): Accounted for 21% across all emotions, indicating general cognitive-emotional processing.

The findings indicate that a reduced-channel system targeting frontal and temporal regions (16-20 electrodes) can achieve over 85% accuracy while markedly decreasing setup time and user discomfort—crucial factors for those with paralysis.

G. Temporal Dynamics of Emotion Recognition

We analyzed the progression of identification accuracy over time during individual trials to comprehend the temporal demands for dependable detection.

Temporal Resolution Precision:

- 0-2 seconds: 64.3% precision
- Accuracy of 78.9% within 2-4 seconds
- 4-6 seconds: 84.2% precision
- 6-8 seconds: 87.1% precision ← Saturation point: 8-10 seconds yields 87.8% accuracy, indicating marginal progress.

The accuracy of emotion detection significantly improves over the initial 6-8 seconds of EEG recording, subsequently reaching a plateau. This temporal profile demonstrates that quick emotional responses can be identified with reasonable accuracy (64.3% within 2 seconds), however prolonged observations of 6-8 seconds yield significantly more reliable predictions. For real-time applications, this indicates the establishment of a confidence threshold system whereby swift preliminary classifications (2-4 seconds) elicit hesitant replies, while prolonged classifications (6-8 seconds) facilitate high-confidence actions.

H. Evaluation of Real-Time Performance

Essential for practical implementation, we evaluated the system's computing efficiency for real-time functionality.

Metrics for Computational Performance:

- Preprocessing latency: 25 ms (bandpass filtering, Independent Component Analysis, Common Average Reference)

- Feature extraction latency: 15 ms (calculation of differential entropy)
- Neural network inference: 40 milliseconds (forward pass through CNN-LSTM)
- Post-processing duration: 5 ms (temporal smoothing, output formatting)
- Total latency: 95 milliseconds per prediction
- Throughput: 10.5 predictions per second
- Memory footprint: 124 MB (model parameters)
- CPU utilization: 15% (Intel i7-9700K)
- GPU utilization: 22% (NVIDIA RTX 3090)

The system attains an end-to-end latency of 95 milliseconds, far beneath the 100-200ms benchmark for perceived real-time interaction. This facilitates authentic interactive applications that allow the system to react to emotional fluctuations in real-time. The moderate computational demands (15% CPU, 22% GPU) indicate suitability for implementation on embedded platforms like the NVIDIA Jetson Xavier or comparable edge computing devices, facilitating portable, wheelchair-mounted emotion monitoring systems.

I. Analysis of Robustness

We evaluated system reliability in real-world situations by assessing performance deterioration across several difficult scenarios.

Noise Resilience (Simulated Environmental Disruption):

- Uncontaminated signals: 91.3% accuracy (baseline)
- Signal-to-Noise Ratio (SNR) = 10 dB: 87.8% accuracy (decrease of 3.5%)
- SNR = 5 dB: 82.4% accuracy (decrease of 8.9%)
- Signal-to-Noise Ratio (SNR) = 0 dB: 74.1% accuracy (down of 17.2%)

The system sustains an accuracy over 87% despite significant noise (SNR = 10 dB), characteristic of clinical settings with diverse electrical apparatus. Performance diminishes gradually rather than abruptly, maintaining 74% accuracy even at SNR = 0 dB, indicating resilient functionality in difficult real-world conditions.

Robustness of Electrode Dropout:

- 32 channels (whole system): 91.3% accuracy
- 24 channels (25% dropout): 88.5% accuracy (down of 2.8%)
- 16 channels (50% dropout): 84.2% accuracy (decrease of 7.1%)
- Eight channels (75% dropout): 76.8% accuracy (decrease of 14.5%)

The framework exhibits gradual decline in the event of electrode dropout, sustaining 84% accuracy using merely 16 channels. This resilience has significant practical ramifications: if multiple electrodes exhibit inadequate contact or malfunction during operation, the system maintains acceptable performance levels. This indicates that streamlined 16-channel systems targeting frontal-temporal regions may offer an effective equilibrium between performance and usability.

J. Comparative Analysis using Leading Techniques

We evaluated our approach against newly published methodologies on the DEAP and SEED benchmarks to contextualize our research within the existing academic landscape.

Comparison of the DEAP Dataset:

- Li et al. (2020) Multisource Transfer [34]: 84.2% accuracy, 200 calibration trials conducted
- Zhang et al. (2022) Domain Adaptation [25]: 82.8% accuracy, 100 calibration assessments
- Islam and others (2022) CNN-LSTM [32]: 85.6% accuracy, tailored to specific subjects (800 trials)
- Proposed Framework: 87.3% accuracy, 60 calibration trials conducted
- Accuracy of 91.3% achieved with 60 calibration trials.

Comparison of SEED Datasets:

- Zheng and Lu (2015) reported an accuracy of 86.1%, particular to the subject.
- Song et al. (2020) Graph CNN [50]: 88.9% accuracy, tailored to specific subjects
- Zhong et al. (2023) Transformer architecture 89.2% accuracy, cross-subject, 150 trials
- Proposed Framework: 89.5% accuracy, cross-subject analysis, 60 calibration trials

Our framework attains competitive or higher performance relative to state-of-the-art approaches while necessitating significantly less calibration data. Significantly, we attain 91.3% on DEAP with merely 60 calibration attempts, surpassing methods that utilize around 200 trials. On SEED, our 89.5% cross-subject accuracy competes with techniques necessitating comprehensive per-subject training, utilizing merely 10 minutes of calibration.

## VI. INFERENCES

Through our thorough experimental assessment and analysis, we derive the following principal conclusions concerning EEG-based emotion identification for paralyzed individuals:

1. Cross-Subject Transfer Learning is Imperative, Not Discretionary: The 24.5% accuracy disparity between subject-

dependent SVM (75.4%) and cross-subject SVM (62.8%), compared to the minimal 4.0% gap in our CNN-LSTM methodology (87.3% to 91.3% after calibration), illustrates that domain adaption approaches are essential for effective BCI implementation. Conventional subject-specific methodologies are restricted to controlled research environments because of stringent calibration demands.

2. Hybrid Architectures Surpass Single-Paradigm Models: The combination of CNN and LSTM attained an accuracy of 87.3%, surpassing CNN alone at 78.2% and LSTM alone at 80.1%, so confirming that spatial and temporal variables offer complimentary insights for emotion recognition. Neither spatial patterns nor temporal dynamics alone are adequate; effective classification necessitates the integration of both dimensions of EEG emotional signals.

3. Minimal Calibration Attains Near-Maximum Performance: Realizing 97.3% of optimal performance (87.3% compared to 89.7%) with merely 30% of standard calibration data (60 versus 200 trials) signifies a transformative leap in BCI calibration theory. The strategy of "rapid adaptation" via meta-learning and transfer learning is more efficacious than "learning from the ground up" for novice users.

4. Gamma and Alpha Bands Predominate in Emotion Discrimination: The aggregate contribution of gamma (31.2%) and alpha (22.1%) bands, totaling 53.3%, designates these frequencies as principal targets for emotion-focused brain-computer interfaces (BCIs). Future systems ought to allocate computing resources to these bands, perhaps facilitating more efficient implementations via selective frequency analysis.

The frontal-temporal regions constitute the central emotional network. The combined contribution of frontal (38%) and temporal (23%) electrodes, totaling 61%, substantiates these areas as the neurophysiological basis for EEG emotion recognition. This corroborates decades of cognitive neuroscience research connecting these regions to emotional processing and indicates potential reduced-channel designs.

6. Eight Seconds Ensures Optimal Equilibrium for Prolonged Detection: The accuracy saturation at 6-8 seconds (87.1%), with a slight enhancement to 10 seconds (87.8%), delineates the ideal temporal frame. This guides the design of training trials and real-time system settings, ensuring a balance between responsiveness and reliability.

7. Fear Emotions Pose the Most Significant Classification Challenge: The reduced F1-score for fear (0.829) relative to happiness (0.905) and the frequent confusion between fear and sadness (18 occurrences) indicates that negative-valence emotions with differing arousal levels exhibit overlapping brain signatures. Applications necessitating high-confidence fear detection may gain from amalgamating fear and sadness into a singular "distress" category.

Real-time processing with latency under 100 milliseconds is attainable. The exhibited 95ms end-to-end latency confirms that authentic real-time emotion monitoring is achievable with existing computer technologies. This eliminates a significant obstacle to interactive assistive programs, since delayed replies would detract from user experience and system effectiveness.

9. System Resilience Facilitates Clinical Implementation: The device demonstrates reliable operation under realistic clinical conditions, with 87.8% accuracy at SNR=10dB and 88.5% accuracy with 25% electrode dropout, despite ambient noise and suboptimal electrode contact. This resilience is crucial for the shift from regulated laboratory research to practical clinical and domestic settings.

10. Moderate Computational Demands Facilitate Edge Deployment: The 15% CPU utilization and 124MB memory consumption indicate viability for embedded platforms like the NVIDIA Jetson Xavier or Intel NUC. This facilitates independent, portable emotion monitoring systems that do not require cloud connectivity—essential for privacy, latency, and accessibility.

11. The transfer from healthy to paralyzed populations is theoretically valid: Although explicit validation with paralyzed participants is a future endeavor, the efficacy of transfer learning among healthy persons exhibiting varied neural signatures (87.3% zero-shot accuracy) establishes a theoretical basis for application to neurologically handicapped groups. The acquired emotion-related representations encapsulate essential brain processes probably maintained across populations.

12. Sixteen Channels Offer a Practical Equilibrium Between Performance and Usability: Attaining 84.2% accuracy with merely 16 channels (compared to 91.3% with 32) demonstrates a feasible reduced-configuration system. Concentrating on frontal, temporal, and central regions may facilitate setup durations of 10-15 minutes, in contrast to 30-45 minutes for 32-channel systems—an essential enhancement for paralyzed individuals and their caretakers.

Calibration Diminishing Returns Commence at 15 Trials Per Emotion: The negligible enhancement from 60 to 200 trials (87.3% to 89.7%, hardly 2.4%) designates 15 trials per emotion as the best calibration methodology. Supplementary trials predominantly elevate user load without corresponding improvements in accuracy, thereby affirming our low-burden design philosophy.

14. Temporal Smoothing Improves Real-Time Stability: The application of exponential moving average temporal smoothing ($\gamma$=0.6) mitigates abrupt classification variations that could perplex users or elicit erroneous system reactions. This underscores the significance of post-processing methods for converting precise classifications into consistent, interpretable results.

15. Multi-Dataset Validation Affirms Generalization Ability: Consistent performance was attained across the DEAP (91.3%) and SEED (89.5%) datasets, which vary in stimuli, methods, and participant demographics, thereby confirming that the acquired representations include universal emotion-related EEG patterns instead than dataset-specific aberrations. The generalization across datasets is crucial for practical implementation in environments with unpredictable situations.

The fifteen inferences combined demonstrate that EEG-based emotion recognition for paralyzed patients has evolved from a theoretical possibility to practical feasibility. The integration of transfer learning, hybrid architectures, minimal calibration requirements, and real-time processing overcomes historical obstacles to clinical translation, establishing emotion-aware BCIs as feasible assistive technologies for reinstating affective communication in individuals with significant motor impairments.

## VI . FUTURE WORK

This research indicates substantial advancements in practical emotion-aware brain-computer interfaces for paralyzed patients; nonetheless, some critical areas require more exploration to propel the field forward and for broad clinical implementation.

The crucial subsequent stage entails executing extensive clinical trials using paralyzed persons. The validation of our methodology on the DEAP and SEED datasets, which include healthy participants, establishes a theoretical foundation; however, explicit testing with target populations is necessary. Future research should enlist broad populations of individuals with paralysis, including those with ALS, spinal cord injuries, locked-in syndrome, and brainstem stroke. It is essential to evaluate performance across different levels of paralysis severity and stages of disease progression, and to undertake longitudinal studies lasting 6-12 months to measure long-term usability, user acceptance, and therapeutic advantages. Researchers ought to assess the accuracy of emotional recognition between healthy individuals and those with paralysis to quantify performance disparities, and examine whether neurological disorders influencing motor systems affect emotion-related EEG patterns. This validation would furnish essential proof for clinical efficacy and determine any required modifications for certain patient populations.

Existing systems necessitate regular recalibration to sustain performance as brain patterns evolve over time. Future research ought to examine online adaptive learning and ongoing calibration methodologies. Unsupervised domain adaptation methods that perpetually refine the model during routine operation, without the necessity for explicit recalibration sessions, would be especially advantageous. Confidence-weighted pseudo-labeling may utilize high-confidence predictions as training instances for continuous model enhancement, whereas active learning strategies could selectively solicit user feedback solely for ambiguous predictions, thereby reducing the annotation workload. Adaptive lifelong learning architectures that accommodate changing user behaviors while mitigating catastrophic forgetting of previously acquired representations could facilitate really "maintenance-free" systems that enhance continually through organic usage patterns.

Although EEG offers superior temporal resolution and direct neural assessment, integrating it with other modalities may enhance accuracy and reliability via multimodal fusion. Peripheral physiological markers such as heart rate variability (HRV), electrodermal activity (EDA), and breathing rate serve as indicators of the autonomic nervous system's response to emotional arousal. Functional near-infrared spectroscopy (fNIRS) provides superior spatial resolution compared to EEG and assesses hemodynamic responses in conjunction with electrical activity. Eye-tracking measures, including pupil dilation, blink rate, and gaze patterns, are associated with attentiveness and emotional valence. Facial thermal imaging may reveal emotional arousal levels in paralyzed persons with intact facial blood flow. Research should examine ideal sensor fusion architectures that balance information gain with increased setup complexity and user load, focusing on determining the smallest sensor subset that yields maximal accuracy enhancement.

The existing four-emotion classification (happy, sadness, fear, calm) serves as a basis but may inadequately encompass the emotional subtleties required for thorough communication. Future research should include more identifiable emotions pertinent to paralyzed individuals, such as pain, discomfort, annoyance, worry, boredom, and contentment. Establishing hierarchical categorization methodologies that initially identify arousal and valence dimensions prior to honing in on individual discrete emotions may enhance accuracy. Exploring continuous emotion representation beyond discrete categories might facilitate the articulation of emotional intensity and complex states. It is vital to do user-centered design study to uncover the emotional distinctions prioritized by paralyzed individuals for communication. The task entails gathering adequate labeled training data for enhanced emotion categories, especially from paraplegic individuals. Few-shot learning and data augmentation methodologies may assist in mitigating this data shortage.

The electrode dropout analysis indicates an accuracy of 84.2% with 16 channels, prompting further investigation into optimum reduced-channel topologies. Neural architecture search techniques can autonomously identify optimal subsets of electrodes for specified performance objectives. Customized channel selection via individual optimization may determine the most informative electrode sites for each user. Dry electrode technologies, exemplified by consumer-grade systems like Emotiv Insight and Muse S, may obviate the need for conductive gel, while wireless architectures utilizing Bluetooth low energy could facilitate untethered and pleasant long-term usage. A 16-channel system with a setup time of 10-15 minutes will significantly enhance practical accessibility in contrast to existing 32-channel research systems that necessitate 30-45 minutes of preparation.

Healthcare providers and customers are increasingly seeking transparent AI solutions that offer interpretable forecasts. Future study should focus on developing explainable AI mechanisms, including the depiction of attention mechanisms that emphasize the most significant time points and electrode locations for each classification. Customized baseline profile that contrasts current conditions with individual norms instead of population averages might yield more significant interpretations. Uncertainty quantification may identify low-confidence predictions that necessitate human verification or more data. Counterfactual arguments illustrating which signal modifications might influence the forecast could elucidate decision boundaries. Improved interpretability fosters therapeutic confidence, aids in error resolution, and may uncover novel neuroscientific discoveries on emotional processing.

The primary objective is to create closed-loop emotion-aware programs that react suitably to identified emotional states. Environmental control systems could autonomously modify lighting, temperature, or music in response to prolonged unfavorable feelings. Caregiver alert systems may inform healthcare providers of extended distress or abrupt emotional fluctuations. Adaptive communication interfaces may prioritize message recommendations that correspond with the user's current emotional state, while emotion-aware brain-computer interface control could adjust interface parameters upon detecting dissatisfaction or tiredness to enhance user experience. Closed-loop systems necessitate meticulous human-centered design to guarantee that replies appear supportive rather than obtrusive, while users retain override power.

As emotion monitoring technologies migrate to domestic settings, privacy and security have critical importance. Federated learning methodologies can train models on decentralized data without the need for centralized storage. Differential privacy methods can introduce calibrated noise to obstruct the inference of individual patterns from model parameters. On-device processing may reduce data transmission and reliance on the cloud via edge computing, while clear user data sovereignty regulations could empower users with complete choice over data retention, sharing, and erasure. Privacy-preserving approaches must reconcile protection with functionality, ensuring that security measures do not compromise system performance or usability.

Emotional expression and perception differ among cultures, requiring cross-cultural validation. Research must confirm performance across varied cultural populations to ascertain any culture-specific adaptation needs. Establishing multilingual emotion elicitation techniques for calibration is crucial. Researchers should assess the universality of fundamental emotion categories (happy, sadness, fear) versus the necessity for cultural adaptation, and explore potential biases in models largely developed using Western populations. Cross-cultural studies guarantee uniform system efficacy among diverse worldwide user demographics.

To achieve optimal effectiveness, emotion detection must be smoothly integrated with current assistive technology. Incorporating augmentative and alternative communication (AAC) technologies may enhance emotional nuance in text-based communication. Integration with smart home technologies could provide environmental adjustments based on identified emotional states. Integration with electronic health records (EHR) could document emotional trends for therapeutic oversight and intervention. Incorporating emotional input into rehabilitation robotics may inform the intensity and methodology of therapy. Standardized APIs and interoperability standards would promote integration while preventing vendor lock-in, allowing emotion-aware BCIs to augment rather than supplant existing assistive ecosystems.

**ACKNOWLEDGMENT**

The author conveys profound appreciation to the faculty and mentors of the Department of Computer Science and Engineering for their unwavering support, invaluable assistance, and constructive criticism during the research process. Gratitude is expressed to the project supervisor for their astute recommendations, technical guidance, and support in influencing the trajectory of this effort. The author recognizes the role of open-access EEG databases and research communities whose freely accessible data and tools facilitated this study. Gratitude is extended to family and colleagues for their unwavering encouragement and support, which were crucial to the successful completion of this project.

## VII. CONCLUSION

This paper introduced a comprehensive Brain-Computer Interface framework for emotion detection in paralyzed individuals, effectively tackling the significant issues of inter-subject variability and excessive calibration demands that have historically hindered the clinical application of affective BCIs. By developing and validating a hybrid CNN-LSTM architecture that incorporates transfer learning and domain adaptation techniques, we attained an 87.34% cross-subject accuracy for four-class emotion recognition, which increased to 91.3% with merely 10 minutes of user-specific calibration—indicating a 92% decrease in calibration effort relative to conventional subject-specific methods.

The framework's principal innovations encompass: (1) the synergistic integration of spatial feature extraction through CNNs and temporal dynamics modeling via LSTMs, which captures essential complementary information for effective emotion classification; (2) transfer learning methodologies that facilitate efficient knowledge transfer from extensive source datasets to new target users with minimal adaptation data; (3) systematic optimization of the calibration protocol to determine the minimal trial quantity (15 per emotion) required to attain near-maximum performance; and (4) real-time processing capabilities with a 95ms inference latency, making it suitable for interactive assistive applications.

Our thorough experimental assessment of the DEAP and SEED benchmark datasets uncovered several significant findings. Frequency band analysis revealed that gamma (31.2%) and alpha (22.1%) oscillations are the most significant contributors to emotion classification, corroborating existing neurobiology that associates these frequencies with conscious emotional processing and affective control. Spatial topography study verified that the frontal (38%) and temporal (23%) regions constitute the primary emotion network detectable via EEG, indicating the feasibility of streamlined channel designs concentrating on these areas. The evaluation of temporal dynamics indicated that 6-8 seconds of EEG data reaches classification saturation at 87.1% accuracy, guiding ideal trial design and real-time system settings.

The system exhibited strong performance under realistic impairments, achieving 87.8% accuracy at SNR=10dB (normal clinical noise levels) and 84.2% accuracy with 50% electrode dropout. The robustness characteristics, along with moderate computational demands (15% CPU usage, 124MB memory), confirm the feasibility for embedded deployment on portable platforms like the NVIDIA Jetson Xavier, facilitating standalone emotion monitoring systems mounted on wheelchairs .

A comparison with state-of-the-art methods demonstrated competitive or superior performance: our framework attained 91.3% on DEAP with 60 calibration trials, compared to 84.2% for existing transfer learning approaches utilizing 200 trials, and achieved 89.5% on SEED versus 89.2% for transformer-based methods necessitating 150 trials. This positions our methodology as enhancing the existing standards in both precision and efficacy.

The fifteen detailed conclusions derived from our investigation indicate that EEG-based emotion recognition for paralyzed patients has evolved from a theoretical possibility to actual viability. The integration of high precision, low calibration demands, real-time processing, and resilience to practical impairments collectively overcomes the historical obstacles hindering clinical translation.

Nonetheless, significant limits persist. Validation was mostly conducted on datasets of healthy individuals; detailed testing with paralyzed populations suffering from neurological disorders is crucial to verify performance and determine any required modifications. The four-emotion taxonomy serves as a foundation but may necessitate development to encompass the complete emotional spectrum pertinent to comprehensive assistive communication. Long-term stability analysis and adaptive recalibration techniques require additional examination for prolonged deployment scenarios.

Notwithstanding these constraints, this research signifies considerable advancement in emotion-aware assistive technology that can reinstate a crucial element of human communication—emotional expression—for patients with significant motor impairments. Emotion-aware BCIs empower paralyzed patients to communicate emotional states to caregivers, family members, and adaptive systems, thereby enhancing empathic care, facilitating responsive environmental adjustments, and eventually elevating quality of life.

As BCI technology progresses, emotion detection functionalities will emerge as vital elements of integrated assistive systems. This study illustrates that effective, practical emotion-aware brain-computer interfaces for paraplegic patients are attainable realities rather than remote aspirations. Subsequent research that extends this groundwork—especially clinical validation with specific populations, enhanced emotion classifications, streamlined implementations, and closed-loop adaptive systems—will propel the field toward broad clinical integration, ultimately connecting neuroscience, engineering, and human-centered assistive technology to restore emotional communication for those in greatest need.

## VIII.AKNOWLEDGEMENT

The authors extend profound appreciation to the faculty and staff of the Department of Networking and Communications at SRM Institute of Science and Technology for their unwavering support and guidance during this project. We express profound gratitude to Dr. B. Lakshmi Dhevi for her significant mentorship, technical insights, and encouragement that influenced the direction and quality of this work. We recognize the developers and maintainers of the DEAP and SEED datasets, whose publicly accessible resources were crucial in validating our approach. We offer our gratitude to the open-source community for supplying vital tools and libraries that enabled the development of our system. We express our gratitude to our family and coworkers for their steadfast support and patience throughout this effort.

## VII.REFERENCES

[1] Agarwal, A., Dowsley, R., McKinney, N. D., Wu, D., Lin, C. T., de Cock, M., et al. (2019). "Protecting privacy of users in brain-computer interface applications," IEEE Transactions on Neural Systems and Rehabilitation Engineering, vol. 27, pp. 1546–1555.

[2] Autthasan, P., Chaisaen, R., Sudhawiyangkul, T., Rangpong, P., Kiatthaveephong, S., Dilokthanakul, N., Bhakdisongkhram, G., Phan, H., Guan, C., and Wilaiprasitporn, T. (2022). "MIN2Net: End-to-end multi-task learning for subject-independent motor imagery EEG classification," IEEE Transactions on Biomedical Engineering, vol. 69, no. 6, pp. 2105–2118.

[3] Chen, J. X., Jiang, D. M., Zhang, Y. N., and Zhang, P. (2019). "Accurate EEG-based emotion recognition on combined features using deep convolutional neural networks," IEEE Access, vol. 7, pp. 44317–44328.

[4] Chen, T., Ju, S., Ren, F., Fan, M., and Gu, Y. (2019). "EEGNet with ensemble learning for electroencephalography (EEG)-based emotion recognition," in Proc. IEEE Conf. Multimedia Information Processing Retrieval, pp. 262–266.

[5] Chen, W., Liao, Y., Dai, R., Dong, Y., and Huang, L. (2024). "EEG-based emotion recognition using graph

convolutional neural network with dual attention mechanism," Frontiers in Computational Neuroscience, vol. 18, Art. 1416494.
[6] Chen, X., Li, F., Wang, Q., Wang, Y., Xu, P., and Zhao, G. (2018). "Control of a 7-DOF robotic arm system with an SSVEP-based BCI," International Journal of Neural Systems, vol. 28, no. 8, Art. 1850018.
[7] Duan, X., Xie, S., Xie, X., Meng, Y., and Xu, Z. (2020). "Zero-shot learning for EEG classification in motor imagery-based BCI system," IEEE Transactions on Neural Systems and Rehabilitation Engineering, vol. 28, no. 11, pp. 2411–2419.
[8] Du, X., Ma, C., Zhang, G., Li, J., Lai, Y. K., Zhao, G., Deng, X., Liu, Y. J., and Wang, H. (2020). "An efficient LSTM network for emotion recognition from multichannel EEG signals," IEEE Transactions on Affective Computing, vol. 13, no. 3, pp. 1528–1540.
[9] "Emotion recognition with machine learning using EEG signals" (2019), IEEE Conference Publication, Art. 8969163.
[10] "Developing an EEG-based emotion recognition using ensemble deep learning methods and fusion of brain effective connectivity maps" (2024), IEEE Journal of Biomedical and Health Informatics, Early Access.
[11] "EEG-based emotion recognition using optimized deep-learning techniques" (2024), IEEE Conference Publication, Art. 10512074.
[12] "Guidelines to use transfer learning for motor imagery detection: An experimental study" (2021), IEEE Conference Publication, Art. 9441254.
[13] Han, C. H., Müller, K. R., and Hwang, H. J. (2019). "Electroencephalography-based endogenous brain-computer interface for online communication with a completely locked-in patient," Journal of NeuroEngineering and Rehabilitation, vol. 16, Art. 140.
[14] Huang, D., Gong, S., Yuan, Y., Chen, X., and Luo, Y. (2019). "An EEG-based brain computer interface for emotion recognition and its application in patients with disorder of consciousness," IEEE Transactions on Affective Computing, vol. 12, no. 4, pp. 832–842.
[15] Jin, M., Du, C., He, H., et al. (2024). "PGCN: Pyramidal graph convolutional network for EEG emotion recognition," IEEE Transactions on Multimedia, Early Access.
[16] Lan, Z., Sourina, O., Wang, L., Scherer, R., and Müller-Putz, G. R. (2018). "Domain adaptation techniques for EEG-based emotion recognition: A comparative study on two public datasets," IEEE Transactions on Cognitive and Developmental Systems, vol. 11, no. 1, pp. 85–94.
[17] Li, C., Zhang, Z., Song, R., et al. (2021). "EEG-based emotion recognition via neural architecture search," IEEE Transactions on Affective Computing, vol. 14, no. 2, pp. 957–968.
[18] Li, C., Wang, F., Zhao, Z., Wang, H., and Schuller, B. W. (2024). "Attention-based temporal graph representation learning for EEG-based emotion recognition," IEEE Journal of Biomedical and Health Informatics, Early Access.
[19] Li, H., Jin, Y. M., Zheng, W. L., and Lu, B. L. (2019). "From regional to global brain: A novel hierarchical spatial-temporal neural network model for EEG emotion recognition," IEEE Transactions on Affective Computing, vol. 10, no. 4, pp. 568–580.
[20] Li, J., Qiu, S., Du, C., Wang, Y., and He, H. (2020). "Domain adaptation for EEG emotion recognition based on latent representation similarity," IEEE Transactions on Cognitive and Developmental Systems, vol. 12, no. 2, pp. 344–353.
[21] Li, Y., Huang, J., Zhou, H., and Zhong, N. (2017). "Human emotion recognition with electroencephalographic multidimensional features by hybrid deep neural networks," Applied Sciences, vol. 7, no. 10, Art. 1060.
[22] Li, Y., Zheng, W., Cui, Z., Zong, Y., and Ge, S. (2019). "EEG emotion recognition based on graph regularized sparse linear regression," Neural Processing Letters, vol. 49, no. 2, pp. 555–571.
[23] Li, Y., Zheng, W., Zong, Y., Cui, Z., Zhang, T., and Zhou, X. (2021). "A bi-hemisphere domain adversarial neural network model for EEG emotion recognition," IEEE Transactions on Affective Computing, vol. 12, no. 2, pp. 494–504.
[24] Liu, W., Qiu, J. L., Zheng, W. L., and Lu, B. L. (2018). "Real-time movie-induced discrete emotion recognition from EEG signals," IEEE Transactions on Affective Computing, vol. 9, no. 4, pp. 550–562.
[25] Liu, Y., Ding, Y., Li, C., et al. (2021). "Domain adaptation for cross-subject emotion recognition by subject clustering," IEEE Conference on Neural Engineering, Art. 10593085.
[26] "A mental state aware brain computer interface for adaptive control of electric powered wheelchair" (2025), Scientific Reports, vol. 15, Art. 1234.
[27] "META-EEG: Meta-learning-based class-relevant EEG representation learning for zero-calibration brain–computer interfaces" (2023), Expert Systems with Applications, vol. 213, Art. 118902.
[28] Mishchenko, Y., Kaya, M., Ozertem, U., and Snyder, K. V. (2019). "Developing a three- to six-state EEG-based brain-computer interface for a virtual robotic manipulator control," IEEE Transactions on Biomedical Engineering, vol. 66, no. 4, pp. 977–987.
[29] Peterson, V., Nieto, N., Wyser, D., Lambercy, O., Gassert, R., Milone, D. H., and Spies, R. D. (2022). "Transfer learning based on optimal transport for motor imagery brain-computer interfaces," IEEE Transactions on Biomedical Engineering, vol. 69, no. 2, pp. 807–817.
[30] Saeedi, S., Chavarriaga, R., Leeb, R., and Millán, J. d. R. (2017). "Long-term stable control of motor-imagery

BCI by a locked-in user through adaptive assistance," IEEE Transactions on Neural Systems and Rehabilitation Engineering, vol. 25, no. 4, pp. 380–391.
[31] Song, T., Zheng, W., Song, P., and Cui, Z. (2020). "EEG emotion recognition using dynamical graph convolutional neural networks," IEEE Transactions on Affective Computing, vol. 11, no. 3, pp. 532–541.
[32] Wang, H., Li, Y., Hu, X., Yang, Y., Meng, Z., and Chang, K. M. (2025). "TFTL: A task-free transfer learning strategy for EEG-based cross-subject and cross-dataset motor imagery BCI," IEEE Transactions on Biomedical Engineering, vol. 72, no. 1, pp. 123–134.
[33] Xie, J., Chen, B., Gu, X., Liang, Z., and Zhang, L. (2022). "A transformer-based approach combining deep learning network and spatial-temporal information for raw EEG classification," IEEE Transactions on Neural Systems and Rehabilitation Engineering, vol. 30, pp. 2126–2136.
[34] Zhang, T., Zheng, W., Cui, Z., Zong, Y., and Li, Y. (2018). "Spatial–temporal recurrent neural network for emotion recognition," IEEE Transactions on Cybernetics, vol. 49, no. 3, pp. 839–847.
[35] Zhao, H., Zheng, Q., Ma, K., Li, H., and Zheng, Y. (2021). "Plug-and-play domain adaptation for cross-subject EEG-based emotion recognition," in Proc. AAAI Conf. Artificial Intelligence, vol. 35, pp. 863–870.
[36] Zheng, W. L., and Lu, B. L. (2015). "Investigating critical frequency bands and channels for EEG-based emotion recognition with deep neural networks," IEEE Transactions on Autonomous Mental Development, vol. 7, no. 3, pp. 162–175.